SACLANTCEN REPORT
serial no: SR- 355

# SACLANT UNDERSEA RESEARCH CENTRE REPORT

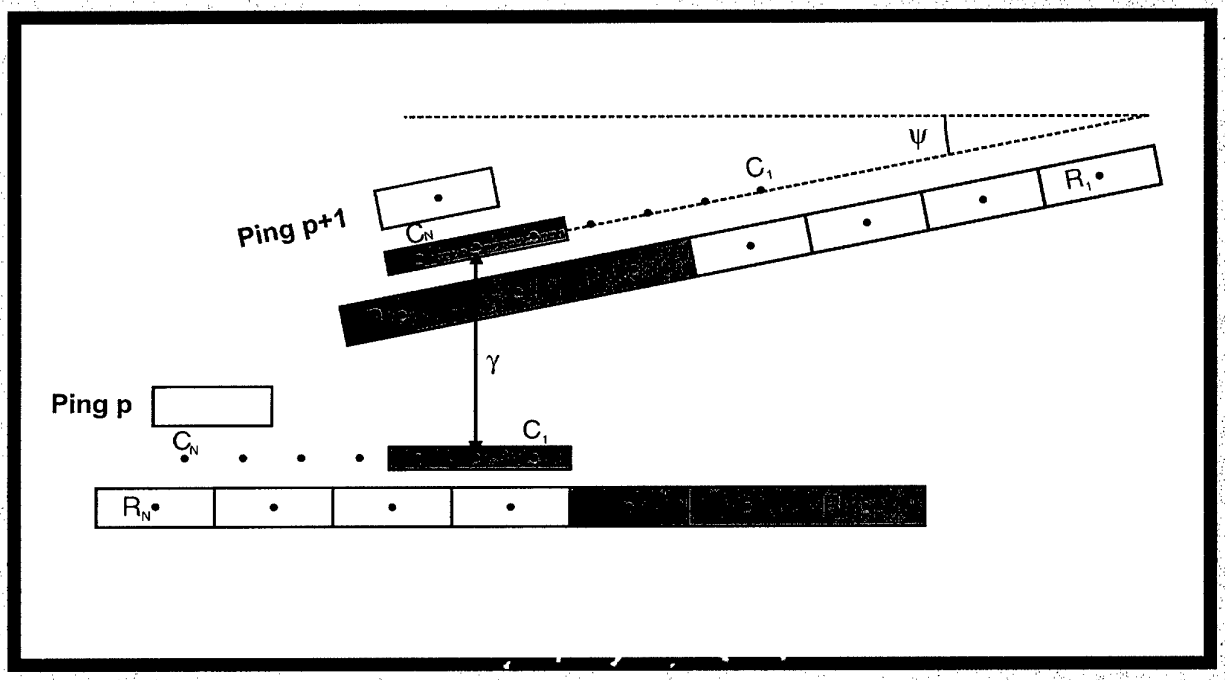




NORTH ATLANTIC TREATY ORGANIZATION ORGANISATION DU TRAITE DE L'ATLANTIQUE NORD

# Accuracy of Synthetic Aperture Sonar Micronavigation using a Displaced Phase Centre Antenna: Theory and Experimental Validation

A. Bellettini, M.A. Pinto

---

The content of this document pertains to work performed under Project 03-G of the SACLANTCEN Programme of Work. The document has been approved for release by The Director, SACLANTCEN.

Jan L. Spoelstra
Director

**Accuracy of Synthetic Aperture Sonar Micronavigation using a Displaced Phase Centre Antenna: Theory and Experimental Validation**

A. Bellettini, M.A. Pinto

**Executive Summary:**

Higher resolution sonars will be required to detect and more importantly to classify mines, which are undetectable by existing sonars, for reasons of shape, material, size or location. Synthetic aperture sonar (SAS) will increase the sonar cross-range resolution by several orders of magnitude while maintaining or increasing the area search rate and thus contribute to an enhancement of mine hunting performance, in particular in shallow water, where smaller mines are more effective. The side scan configuration of SAS makes it well suited to remotely operated underwater vehicles, such as those forseen for covert survey and reconnaissance operations.

SAS performance is limited by the precision with which the motion errors of the platform can be estimated. The terminology of "micronavigation" is used to describe this very specific requirement for sub-wavelength short-term relative positioning. The aim of this work is to quantify the theoretical performance of data-driven micronavigation based on the displaced phase centre antenna (DPCA) concept, extending the results obtained in Saclantcen memorandum SM-352. The unique feature of DPCA, of great practical significance, is that it does not require the presence of seafloor features as it exploits the spatial coherence properties of seafloor reverberation.

intentionally blank page

**Accuracy of Synthetic Aperture Sonar Micronavigation using a Displaced Phase Centre Antenna: Theory and Experimental Validation**

A. Bellettini, M.A. Pinto

**Abstract:** The Cramér-Rao Lower Bounds (CRLBs) on the cross-track translation and rotation of a Displaced Phase Centre Antenna (DPCA) in the slant range plane between two successive pings (known as DPCA sway and yaw in what follows) are computed, assuming statistically homogeneous backscatter. These bounds are validated using experimental data from a 118-182 kHz sonar, showing an accuracy of the order of 20 microns on the ping-to-ping cross-track displacements.

Next, the accuracy required on the DPCA sway and yaw in order to achieve a given SAS beampattern specification, specified by the expected SAS array gain, is computed as a function of the number $P$ of pings in the SAS. Higher accuracy is required when $P$ increases to counter the accumulation of errors during the integration of the elementary ping-to-ping estimates: the standard deviation must decrease as $P^{-1/2}$ for the DPCA sway and $P^{-3/2}$ for the yaw.

Finally, by combining the above results, the lower bounds on DPCA micronavigation accuracy are established. These bounds set an upper limit to the SAS length achievable in practice. The maximum gain $Q$ in cross-range resolution achievable by a DPCA micronavigated SAS is computed as a function of the key SAS parameters. It is found that, for $P \gg 1$, the optimum SAS spatial sampling factor is 4, in the sense that it allows maximum $Q$. These theoretical predictions are compared with simulations and experimental results.

# 1

# Introduction

The performance of Synthetic Aperture Sonar (SAS) on ocean going platforms is limited first and foremost by the accuracy with which the motion of the platform can be estimated [1]. The term "micronavigation" is used here to describe this very specific requirement for sub-wavelength short term relative positioning, which is beyond the scope of instrumentation for most high resolution imaging applications. In recent years, data driven micronavigation techniques have emerged as a possible solution. The most promising are based on the concept of Displaced Phase Centre Antenna (DPCA) which exploits, in a unique way, the spatial and temporal coherence properties of the seafloor backscatter [2]. DPCA is a known concept in radar space-time processing [3]. DPCA also forms the basis of correlation sonar, a subject which has recently been revisited theoretically by Doisy [4] who derived the accuracy of translational displacement estimates for volumetric arrays, as well as for attitude-stabilized planar arrays. Several experimental SAS prototypes exploit the DPCA principle for SAS micronavigation [5, 6, 7, 8]. A large data set has been collected with a 100 kHz towed SAS to evaluate DPCA micronavigation for a wide range of parameters [9]. The aim of this work is to determine the theoretical accuracy of DPCA-based SAS micronavigation.

In sections 2 and 3 the basic principles of DPCA are summarized. Next, in section 4, the CRLBs of the DPCA sway and yaw are computed and compared with experimental results. In Section 5, the accuracy required on these quantities in order to achieve a given expected SAS array gain, is computed as a function of the number $P$ of pings in the SAS. In Section 6 the results of Sections 4 and 5 are combined. An effective reverberation to noise ratio $\rho_{\text{eff}}$ is introduced and the maximum gain $Q$ in cross-range resolution achievable by a DPCA micronavigated SAS is computed as a function of $\rho_{\text{eff}}$ and $\alpha$, the SAS spatial sampling factor. It is also shown that, for $P \gg 1$, $\alpha = 4$ is optimum, in the sense that it allows maximum $Q$ for given $\rho_{\text{eff}}$. These theoretical predictions are compared with simulations and experimental results.

# 2

## Phase Centre Approximation

Let $T$ be the position of the transmitter centre at a given sonar ping and $R$ the position of the receiver at the instant of the reception of the echo from an arbitrary scatterer located at $X$ (Fig. 1). The basis of the Phase Centre Approximation (PCA) is to replace the true bistatic situation by a fictitious monostatic one, which assumes transmission and reception occurs from $C = (T + R)/2$.

To see when this is valid, we compute the excess in round trip travel path for the bistatic case over the monostatic one. Let $r = \mathrm{CX}$, $\Delta = \mathrm{TR}$. Expanding in series of $\Delta/r \ll 1$, one obtains:

$$\mathrm{TX} + \mathrm{XR} - 2\ \mathrm{CX} = \frac{\Delta^2}{4r}\cos^2\theta + \frac{\Delta^4}{64r^3}\cos^2\theta(4 - 5\cos^2\theta) + \ldots \qquad (1)$$

where $\theta$ is the bearing of $X$ (Fig. 1).

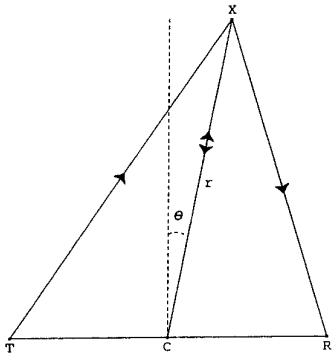


**Figure 1** *Geometry of the Phase Centre Approximation. $T$, $R$, $C$ and $X$ are respectively the positions of the transmitter, receiver, phase centre and single scatterer.*

It is seen that PCA holds when $\Delta^2/4r \ll \lambda_0$, or equivalently $r \gg \Delta^2/4\lambda_0$, which can be interpreted as a far field condition. More generally, PCA also holds in near field at the condition that the received signal is advanced by $\Delta^2/(4rc)$ and the transmission sector satisfies

$$\frac{\Delta^2}{4r\lambda_0}(1 - \cos^2\theta_e) \ll 1 \qquad (2)$$

where $\theta_e$ is the half transmission beamwidth. This condition ensures that the excess

round trip travel path is the same for all scatterers at range $r$ within the 3 dB transmission beamwidth, so that their interference pattern is also the same.

In addition, this derivation has assumed that the bistatic angle $\Delta/r$ is small compared to the beamwidths of both the transmitter and the receiver, so that the corresponding changes in transmission and reception directivity gains between the bistatic case and the monostatic one are negligible. This condition is almost always valid for usual SAS systems.

# 3

## Displaced Phase Centre Antenna

The following analysis of DPCA applies to a multi-element SAS, which consists of a transmitter of length $L_t = d$ and of a receive aperture of $N > 1$ elements spaced at $d$, of total length $L_r = Nd$. Let $T_p$ be the position of the transmitter centre at ping $p$ and $R_{np}$ that of receiving element $n$ at the instant of the reception of the echo from range $r$. Based on PCA this is equivalent to transmission and reception from $C_{np} = (T_p + R_{np})/2$.

The basic idea of DPCA is to cancel the along-track displacement of the sonar between two successive pings by synthesis of an effective displacement, in the opposite direction, of a subset of receiving elements. This is achieved by operating at $D = Md/2$ ($M$ integer), with $M < N$ so that, in the absence of cross-track motion, there are $K = N - M$ phase centres which overlap from ping to ping (see Fig. 2) and which form the DPCA. It follows that the signals of the DPCA are identical for both pings, up to noise and possible changes in the propagation medium or the scatterer geometry.

In the presence of cross-track motion, the cross-track displacements $\gamma_k$ of the $K$ DPCA elements are given, for a small angle $\psi$, by

$$\gamma_k = \gamma + \psi d_k \tag{3}$$

where $\gamma$ and $\psi$ are defined as the DPCA sway[1] and yaw (Fig. 3), and

$$d_k = \left(k - 1 - \frac{K-1}{2}\right)\frac{d}{2} \tag{4}$$

is the abscissa of the phase centre of DPCA element $k$, with respect to the origin taken at the centre of the DPCA.

The cross-track motion leads to a change in round-trip travel path to scatterer $X$ equal to $2\gamma_k \cos\theta$, where $\theta$ is the bearing of $X$. Under the condition that

$$\frac{2\gamma_k}{\lambda_0}(1 - \cos\theta_e) \ll 1 \tag{5}$$

[1]It should be cautioned that the DPCA sway differs from that of the physical array centre in the presence of yaw. The consequences of this will be explicated in Section 5.

the round-trip travel path to all the scatterers within the transmission beam is the same and equal to $2\gamma_k$. It follows that the DPCA signals will again be identical for both pings, up to a delay

$$\tau_k = 2\gamma_k / c \tag{6}$$

which can be estimated by a cross-correlation over a short range window centred at $r$.

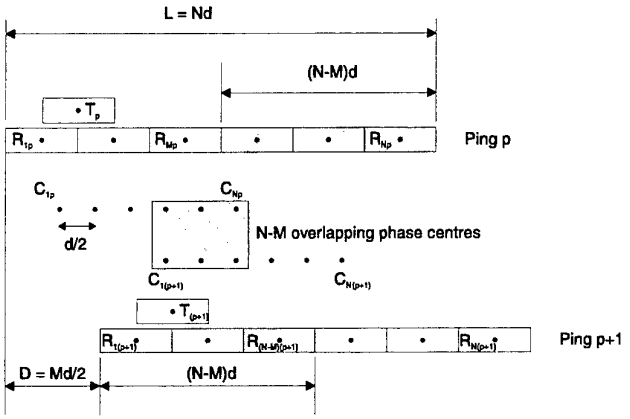


**Figure 2** *Displaced Phase Centre Antenna in the absence of cross-track motion (the upper array has been shifted for clarity).*

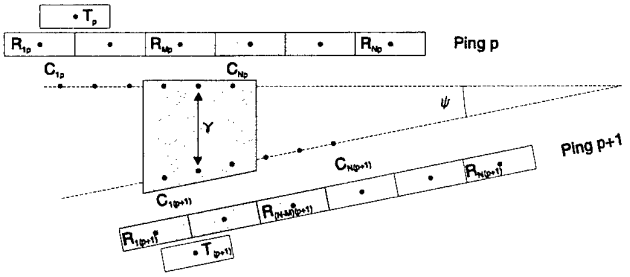


**Figure 3** *DPCA sway $\gamma$ and yaw $\psi$ between successive pings.*

It should be noted that condition (5) limits the maximum cross-track motion. When (5) no longer holds, the DPCA signals decorrelate. This effect has been studied in detail for interferometric sonar, where it is known as "baseline decorrelation" [10].

Furthermore, it has been assumed above that the along-track sonar displacement was known and equal to $Md/2$ with $M$ integer. A standard navigation system could be used for this purpose, together with a system that modifies the ping repetition period to attain the desired spatial sampling, since the accuracy requirements are

not as great as for cross-track motions. Alternatively DPCA can be extended to estimate these quantities as well. However this will not be discussed further here.

By integrating the ping-to-ping displacement estimates provided by the DPCA, the projection of the platform trajectory in the slant-range plane can be reconstructed and used to form the SAS image. Clearly, the finite accuracy of the DPCA will limit the number of pings $P$ which can be summed coherently, possibly to a fraction of the maximum number determined by the transmission beamwidth and range. The corresponding cross-range resolution gain $Q$ achievable in this manner is

$$Q = \frac{L_r + 2(P-1)D}{L_r} = 1 + \frac{P-1}{\alpha} \tag{7}$$

where $\alpha = L_r/2D$ is the SAS spatial sampling factor. The problem posed is the evaluation of the accumulated error of DPCA micronavigation and the limits imposed on the achievable $Q$.

# 4

# Cramér-Rao lower bounds on DPCA sway and yaw

## 4.1 Theory

Let $\{X_1(t), X_1'(t), X_2(t), X_2'(t), ..., X_K(t), X_K'(t)\}$ be the $K$ pairs of signals received by the elements of the DPCA at two successive pings. We will assume that, over the temporal estimation window of duration $W$, these signals can be expressed as

$$X_k(t) = S_k(t) + N_k(t) \tag{8}$$
$$X_k'(t) = S_k(t - \tau_k) + N_k'(t) \tag{9}$$

where the noises $N_k$ and $N_k'$ are mutually independent and independent of the reverberation signals $S_k$. Furthermore, the $S_k$ are assumed independent from each other. This holds because adjacent elements are separated by $d = L_t$, which is the spatial correlation length, for statistically homogeneous reverberation [4]. Finally, reverberation and noise will be assumed to be Gaussian random processes with a flat power spectral density. The reverberation to noise ratio will be denoted by $\rho = \langle S^2 \rangle / \langle N^2 \rangle$.

To compute the CRLBs we proceed to compute the log-likelihood relative to the two parameters $(\gamma, \psi)$ and the corresponding $2 \times 2$ Fisher Information Matrix (FIM). As $(X_k, X_k')$ and $(X_l, X_l')$ are independent for $k \neq l$, this log-likelihood can be expressed as a function of log-likelihood $\mathcal{L}_1(D)$ relative to the estimation of a single delay $D$ as follows:

$$\mathcal{L}_K(\gamma, \psi) = \sum_{1 \leq k \leq K} \mathcal{L}_1(\tau_k(\gamma, \psi)). \tag{10}$$

The required FIM $F_{(\gamma,\psi)}$ can now be obtained directly as a function of $K$ and the FIM of order 1 relative to the estimation of a single delay $\tau$, defined as

$$F_\tau = -\left\langle d^2\mathcal{L}_1/d\tau^2 \right\rangle. \tag{11}$$

One has

$$F_{(\gamma,\psi)} = -\frac{4}{c^2}\left\langle \frac{d^2\mathcal{L}_1}{d\tau^2} \right\rangle \begin{pmatrix} K & \sum d_k \\ \sum d_k & \sum d_k^2 \end{pmatrix}$$

$$= \frac{4}{c^2} F_\tau \begin{pmatrix} K & 0 \\ 0 & \frac{d^2 K(K^2-1)}{48} \end{pmatrix}. \tag{12}$$

The zero non-diagonal terms show that the estimations of $\gamma$ and $\psi$ are separable. The expression of $\sigma_\tau = 1/\sqrt{F_\tau}$ is a result of time delay estimation for passive sonar (see (23) of [11]):

$$\sigma_\tau = \frac{1}{2\pi f_0} \frac{1}{\sqrt{BW}} \sqrt{\frac{1}{\rho} + \frac{1}{2\rho^2}} \tag{13}$$

where $B$ is the signal bandwidth.

The CRLBs can, after some elementary manipulations, be written as:

$$\sigma_\gamma = \frac{1}{2\pi} \frac{\lambda_0}{2} \frac{1}{\sqrt{BW}} \frac{1}{\sqrt{K}} \sqrt{\frac{1}{\rho} + \frac{1}{2\rho^2}} \tag{14}$$

and

$$\sigma_\psi = \frac{\sqrt{3}}{\pi} \sqrt{\frac{K-1}{K+1}} \frac{\lambda_0}{(K-1)d} \frac{1}{\sqrt{BW}} \frac{1}{\sqrt{K}} \sqrt{\frac{1}{\rho} + \frac{1}{2\rho^2}}. \tag{15}$$

The physical interpretation of these formulas is straightforward. The CRLB on $\gamma$ is proportional to $\lambda_0/2$, the half-wavelength at the centre frequency. The CRLB on $\psi$ is proportional to $\lambda_0/(K-1)d$, the angular resolution of the DPCA. Both CRLBs are inversely proportional to the square root of the number $BW$ of independent temporal samples used in the estimation (for statistically homogeneous reverberation) and to that of the number $K$ of independent elements in the DPCA. They both decrease with the reverberation-to-noise ratio $\rho$, as $1/\rho$ for small $\rho$ and $1/\sqrt{\rho}$ for large $\rho$.

The above expressions of the CRLBs show the benefits of operating with wide bandwidth $B$ for DPCA micronavigation, as both DPCA sway and yaw accuracy increase in proportion to $\sqrt{BW}$ due to the increase in the number of independent temporal samples. In addition the yaw accuracy is seen to increase in proportion to $K^{3/2}$, due to the combined effect of the increase (as $K$) in angular resolution of the DPCA and the increase (as $K^{1/2}$) of the number of independent spatial samples. Since

$$K = \frac{L_r - 2D}{L_t} \tag{16}$$

$K$ can be increased by increasing $L_r$, reducing $D$ or reducing $L_t$, i.e. broadening the transmission beam. Ultimately, the transmission beam will be limited by condition (5).

The bounds (14) and (15) were first presented in the open literature by Billon and Fohanno[6].

### 4.2 Experimental validation

It was shown in [8] that the experimental standard deviations approached these CRLBs closely, once the effect of calibration errors of the physical array were removed. A more complete experimental validation is presented in Fig. 4.

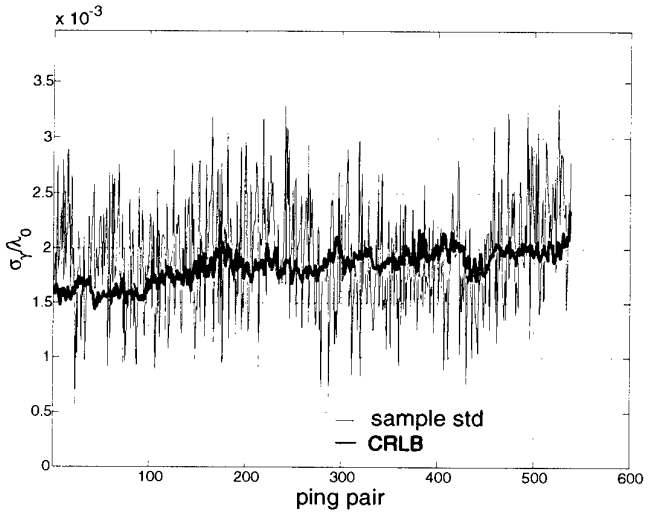


**Figure 4** *Comparison between the theoretical CRLB for a single DPCA element (red) and the experimental sample standard deviation S (black).*

The data were collected in November 2000 at Elba Island (Italy) with a 24 m underwater rail deployed 4 m above a seafloor of sand and rocks. The water depth varied between 13 m and 15 m. The transmitter of length $L_t = 2$ cm had a horizontal beamwidth of 28 deg and a vertical beamwidth of 2.8 deg. The transmitted signal was a 4 ms LFM swept from 118 kHz to 182 kHz, with a ping repetition period of 0.5 s. The receive array had 32 elements spaced at 0.834 cm for a total length $L_r = 26.7$ cm. A constant along-track velocity of 6.675 cm/s was imposed along the rail, giving a SAS spatial sampling factor $\alpha = 4$ and 24 elements in the DPCA.

The DPCA was undersampled by a factor 3, to arrive at 8 independent elements. Estimates $\hat{\gamma}_k$ of $\gamma_k$ ($k = 1, \ldots, 8$) were obtained using a short term correlation with a 5 m long window centred at 45 m range, corresponding to $W = 6.7 \times 10^{-3}$ s and $BW \cong 427$. The reverberation to noise ratio $\rho$, computed from the correlation coefficient $\mu$ as $\rho = \mu/(1-\mu)$ varies between 4.9 dB and 9.5 dB, depending on the ping pair and the DPCA element.

In Fig. 4 the CRLB (14) is plotted as a function of the ping pair, using $BW = 427$, $K = 1$ and the $\rho$ averaged over the 8 DPCA elements. Under the assumption of no yaw during the displacement along the rail, it follows from Eq. (3) that $\hat{\gamma}_1, \ldots, \hat{\gamma}_8$

should be identical up to estimation errors, so that the sample standard deviation $S$ provides an estimate of $\sigma_\gamma$. $S$ is a random variable which, for Gaussian errors, follows a $\chi$-distribution with 7 degrees of freedom. It is shown in Fig. 4 that $S$ is in good agreement with theory. The mean value of the relative estimation error $(S-\sigma_\gamma)/\sigma_\gamma$, obtained averaging over the ping pairs, is only about 6%. Its standard deviation is about 29%, which compares well with the theoretical value of 26% derived from the $\chi$-distribution. The accuracy achieved is of the order of $\lambda_0/500$, which is quite remarkable.

# 5

# Accuracy requirements for DPCA sway and yaw

Let $(O, x, y)$ be the slant range plane, with $Ox$ along-track and $Oy$ across-track, $(x_p, y_p)$ the coordinates of $C_p = (T_p + R_p)/2$, where $R_p$ is the centre of the physical receive aperture at ping $p$, $\theta_p$ the angle between $Oy$ and boresight to the physical aperture.

The trajectory followed by the sonar can be expressed as

$$\begin{cases} x_{p+1} &= x_p + D \\ y_{p+1} &= y_p + \gamma_p + \frac{D}{2}\theta_p + \frac{D}{2}\theta_{p+1} \\ \theta_{p+1} &= \theta_p + \psi_p \end{cases} \tag{17}$$

where $\gamma_p$ and $\psi_p$ are the DPCA sway and yaw between pings $p$ and $p+1$ and the angles $\theta_p$ have been assumed small (Fig. 5).

The quantity $y_{p+1} - y_p$, which can be interpreted as the physical sway between successive pings, is seen to be the sum of three terms. The first is the DPCA sway and the other two result from the heading of the physical reception antenna at pings $p$ and $p+1$. Indeed the geometrical centre of the DPCA and that of the physical array are separated by $D/2$, and this lever arm leads to a difference in cross-track position of the associated phase centres of $D(\theta_p + \theta_{p+1})/2$ (Fig. 5). After algebraic

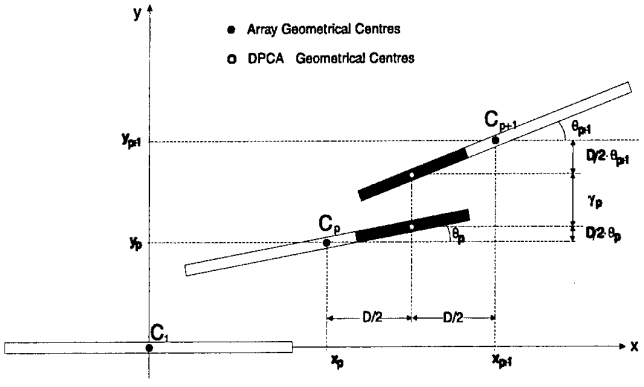


**Figure 5** *SAS trajectory in the slant-range plane.*

manipulations, the estimated trajectory may be expressed as:

$$\begin{cases} x_p &= (p-1)D \\ y_p &= \sum_{l=1}^{p-1} \gamma_l + D \sum_{l=1}^{p-1} \left(p - l - \frac{1}{2}\right) \psi_l \\ \theta_p &= \sum_{l=1}^{p-1} \psi_l. \end{cases} \tag{18}$$

It is important that this trajectory be estimated with sufficient precision. Errors $\delta\gamma_p$ and $\delta\psi_p$ on the DPCA estimates will accumulate to

$$\begin{cases} \delta y_p &= \sum_{l=1}^{p-1} \delta\gamma_l + D \sum_{l=1}^{p-1} \left(p - l - \frac{1}{2}\right) \delta\psi_l \\ \delta\theta_p &= \sum_{l=1}^{p-1} \delta\psi_l. \end{cases} \tag{19}$$

The most important effect for SAS are the cross-track micronavigation errors $\delta y_p$. It is seen in the first equation of (19) that they depend on accumulated errors on the DPCA sway and yaw. In the presence of DPCA sway errors alone ($\delta\psi_p = 0$) they accumulate like a random walk, whereas in the presence of DPCA yaw errors alone ($\delta\gamma_p = 0$) they accumulate like an integrated random walk. In the second case the errors accumulate much faster and lead to a highly correlated pattern of phase errors along the SAS. The quantitative analysis of these errors is presented in what follows.

### 5.1 *Beampattern specification of SAS array factor*

An accuracy study was presented in [6] based on the criterion that the cross-track micronavigation error at the extremity of the SAS, $\delta y_P$, be smaller than $\lambda/8$. This overlooks the fact that linear phase errors steer the SAS array factor, without broadening the SAS mainlobe, so that the term in the $\delta y_p$ which is linear with $p$ must be removed before applying the criterion. After this, the criterion should be similar to the standard one used in SAR for phase errors which vary quadratically over the aperture, which states that a 90 deg phase difference between the centre of the aperture and its extremities leads to a 10% increase in the 3 dB beamwidth.

However, it follows from (19) that if the $\delta y_p$ were expanded as function of $p$, there would certainly be terms of order higher than 2 which are not accounted for in [6]. A more appropriate criterion can be defined using the normalized gain of the SAS array factor which can be expressed as

$$g = \frac{1}{P^2} \left| \sum_{p=1}^{P} \exp(j2k_0(\delta y_p - ap)) \right|^2 \tag{20}$$

where $k_0 = 2\pi/\lambda_0$ is the wavenumber at the centre frequency and

$$a = \sum_{p=1}^{P} \frac{12(p-(P+1)/2)}{P(P^2-1)} \delta y_p \tag{21}$$

is the slope of the linear fit of $\delta y_p$. This criterion extends that of [12] where the linear term had been overlooked.

Subtracting the linear fit accounts for the fact that cross-track micronavigation errors which grow linearly with $p$ simply steer the SAS array factor by $a/D$, without defocusing. However, the steering of the SAS array factor away from the pointing direction of the physical aperture leads to an increase in azimuth ambiguities as well as a loss in reverberation to noise ratio. The peak of the grating lobes will be 20 dB below the mainlobe (see [13] eq. (16)), provided that $a/D \leq \lambda_0/20D$, i.e.,

$$\frac{2a}{\lambda_0} \leq \frac{1}{10}. \tag{22}$$

The SAS beampattern specification will be given in terms of

$$\bar{g} = \langle g \rangle \tag{23}$$

the expected normalized gain of the SAS array factor. For what follows it is also convenient to define a logarithmic gain $G = 10 \log_{10} g$ and correspondingly the expected value $\bar{G}$. Since $0 \leq g \leq 1$, one has $G < 0$.

By elementary algebraic manipulation, Eq. (20) becomes

$$g = \frac{1}{P} + \frac{2}{P^2} \sum_{p=1}^{P} \sum_{q=1}^{p-1} \cos(2k_0(\delta y_p - \delta y_q - a(p-q))) \tag{24}$$

For small errors ($k_0 \delta y_p \ll 1$) Eq. (24) can be expanded in series obtaining the expected gain

$$\bar{g} \simeq 1 - \frac{1}{P^2} \sum_{p=1}^{P} \sum_{q=1}^{p-1} \sigma_{p,q}^2 \tag{25}$$

where

$$\sigma_{p,q}^2 = \left\langle |2k_0(\delta y_p - \delta y_q - a(p-q))|^2 \right\rangle. \tag{26}$$

Since $\delta\gamma_p$ and $\delta\psi_p$ are independent, the corresponding losses in SAS array gain will be studied separately in the next two subsections.

### 5.2 Required DPCA sway accuracy

We assume that $\delta\psi_p = 0$ for all $p$. Then by (19) one has

$$\delta y_p - \delta y_q = \sum_{l=q}^{p-1} \delta\gamma_l \tag{27}$$

and substituting (18) into (21)

$$a = \frac{6}{P(P^2-1)} \sum_{p=1}^{P} p(P-p)\delta\gamma_p. \tag{28}$$

After algebraic manipulations of (25), one finally obtains

$$\bar{g} = 1 - \frac{4\pi^2}{15}(P - \frac{4}{P}) \left(\frac{2\sigma_\gamma}{\lambda_0}\right)^2 \tag{29}$$

where $\sigma_\gamma^2 = \langle \delta\gamma^2 \rangle$. The required accuracy on the DPCA sway can therefore be expressed as a function of $P$ and $\bar{g}$ as:

$$\sigma_\gamma \leq \frac{\lambda_0}{2} \sqrt{\frac{15(1-\bar{g})}{4\pi^2 P}} \qquad (P \gg 1). \tag{30}$$

It is seen that, for given $\bar{g}$, the standard deviation of the DPCA sway estimation is required to decrease as $P^{-1/2}$ for large $P$ (Fig. 6(a)).

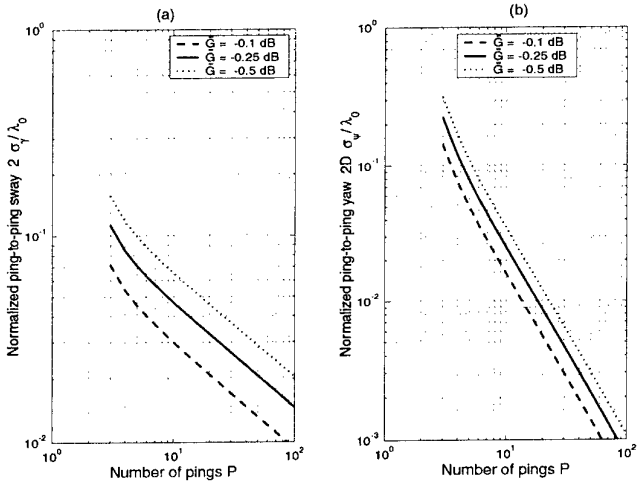


**Figure 6** *Accuracy required on DPCA sway (a) and DPCA yaw (b), to sum coherently P pings in the SAS, for given values of the normalized expected SAS array gain $\bar{G}$.*

Finally, it follows from (28) that

$$\sigma_a = \sqrt{\frac{6}{5P}}\sigma_\gamma \qquad (P \gg 1). \tag{31}$$

where $\sigma_a^2 = \langle a^2 \rangle$. When (30) is substituted into (31), $2\sigma_a/\lambda_0$ decreases as $P^{-1}$ for large $P$. Thus, condition (30) is stronger than (22) and one is justified in specifying the SAS beampattern solely in terms of the SAS array factor.

### 5.3 *Required DPCA yaw accuracy*

We assume $\delta\gamma_p = 0$ for all $p$. Then by (19) one has

$$\delta y_p - \delta y_q = D\sum_{l=1}^{q-1}(p-q)\delta\psi_l + D\sum_{l=q}^{p-1}(p-l-\frac{1}{2})\delta\psi_l \tag{32}$$

and

$$a = D\sum_{p=1}^{P}\frac{(P^2-1+pP-2p^2)(P-p)}{P(P^2-1)}\delta\psi_p \tag{33}$$

After rather cumbersome algebraic manipulations, $\bar{g}$ can be expressed as

$$\bar{g} = 1 - \frac{\pi^2}{105}(P-\frac{4}{P})(P^2-2)\left(\frac{2D\sigma_\psi}{\lambda_0}\right)^2 \tag{34}$$

where $\sigma_\psi^2 = \langle \delta\psi^2 \rangle$.

The required accuracy for the yaw can therefore be expressed as a function of $P$ and $\bar{g}$ as:

$$\sigma_\psi \leq \frac{\lambda_0}{2D}\sqrt{\frac{105(1-\bar{g})}{\pi^2 P^3}} \qquad (P \gg 1). \tag{35}$$

The standard deviation of the DPCA yaw estimation is now required to decrease much faster with $P$ than for the DPCA sway, in proportion to $P^{-3/2}$ for large $P$ instead of $P^{-1/2}$ (Fig. 6(b)).

Finally, it follows from (33) that

$$\sigma_a = \sqrt{\frac{13P}{35}}D\sigma_\psi, \qquad (P \gg 1). \tag{36}$$

When (35) is substituted into (36), $2\sigma_a/\lambda_0$ decreases as $P^{-1}$ for large $P$. Thus, as before, condition (35) is stronger than (22).

# 6

## Required reverberation-to-noise ratio

By combining the results obtained in Sections 4 and 5 it is now possible to find the sonar performance requirements needed to attain a given $Q$. To facilitate the interpretation, it is useful to introduce the effective reverberation to noise ratio

$$\rho_{\text{eff}} = \frac{L_r}{L_t} BW \frac{2\rho^2}{1+2\rho}. \tag{37}$$

For $\rho \gg 1$ this can be interpreted as the product of the reverberation-to-noise ratio $\rho$, the number $L_r/L_t$ of independent elements in the receive aperture and the number $BW$ of independent temporal samples.

The CRLBs (14) and (15) of the DPCA sway and yaw estimators can be then expressed respectively by

$$\sigma_\gamma = \frac{1}{2\pi} \frac{\lambda_0}{2} \sqrt{\frac{\alpha}{\alpha-1}} \frac{1}{\sqrt{\rho_{\text{eff}}}} \tag{38}$$

and

$$\sigma_\psi = \frac{\sqrt{3}}{\pi} \frac{\lambda_0}{2D} \sqrt{\frac{\alpha}{(\alpha-1)^3}} \frac{1}{\sqrt{\rho_{\text{eff}}}} \tag{39}$$

where in the latter it has been assumed $K^2 \gg 1$.

By substituting (38) and (39) into (30) and (35) it is straightforward to obtain the effective reverberation to noise ratios required to limit, respectively, the DPCA sway and yaw errors as a function of $Q$, $\alpha$ and $1-\bar{g}$. In the limit $P \gg 1$, for which (7) becomes $Q - 1 \cong P/\alpha$, they read

$$\rho_{\text{eff}} \geq \frac{Q-1}{15(1-\bar{g})} \frac{\alpha^2}{\alpha-1} \tag{40}$$

$$\rho_{\text{eff}} \geq \frac{(Q-1)^3}{35(1-\bar{g})} \frac{\alpha^4}{(\alpha-1)^3} \tag{41}$$

where it has been assumed that $1-\bar{g} \ll 1$. The required $\rho_{\text{eff}}$ established in [12] was about 11.5 dB higher, due to the omitted linear term in (20).

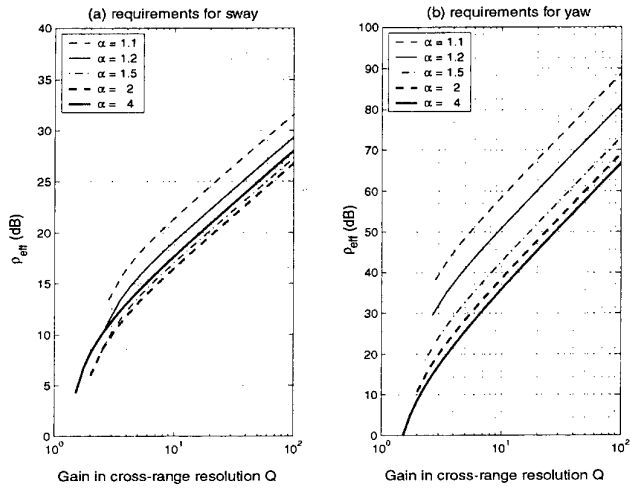


**Figure 7** *Required $\rho_{eff}$ for DPCA sway (a) and DPCA yaw (b), estimated as a function of desired resolution gain $Q$ and SAS sampling factor $\alpha$, for a normalized expected SAS array gain $\bar{G} = -0.25$ dB.*

In Fig. 7 the values of $\rho_{\text{eff}}$ needed to obtain $\bar{G} > -0.25$ dB are plotted as functions of $Q$ and $\alpha$ for the two cases. Figure 7(a) represents the requirements in the limit when only the DPCA sway has to be estimated (i.e. for an infinitely precise independent estimate of the yaw) whereas Fig. 7(b) represents those requirements when both DPCA sway and yaw have to be estimated.

The requirements for accurate DPCA yaw estimation are seen to be higher, by several orders of magnitude, than those for the DPCA sway. Thus the achievable $Q$ by a DPCA micronavigated SAS is limited by estimation errors on the heading of the physical array, which induce cross-track position errors of the physical array in DPCA micronavigation.

The right hand side of (41) attains an absolute minimum for $\alpha = 4$. Therefore, a tradeoff between resolution gain and area mapping rate characterizes the design of a DPCA-micronavigated SAS. According to (41) this tradeoff will usually be in favor of $\alpha < 4$. For fixed $\rho_{\text{eff}}$, the $Q$ obtained with $\alpha = 2$ has a loss of only 16% with respect to the optimal $\alpha$. The loss is much more severe for $\alpha$ approaching 1.

### 6.1 Simulation

To illustrate the preceding analytical results, various realizations of the $\delta y_p$ and corresponding beampatterns were simulated for $Q = 10$, $\alpha = 4$ and $\rho_{\text{eff}} = 35.4$ dB, which correspond to a gain $\bar{G} \cong -0.25$ dB according to (41). The first five realiza-

tions are illustrated in Fig. 8, followed by the reference case with no micronavigation errors. The $\delta y_p$ were obtained by generating independent normal errors $\delta\psi_p$ of zero mean and standard deviation given by the approximate CRLBs (39) for the above values of $\alpha$ and $\rho_{\text{eff}}$ and summing them according to the first equation in (19). It should be noted that the $\delta y_p$ have, as expected, a high degree of correlation.

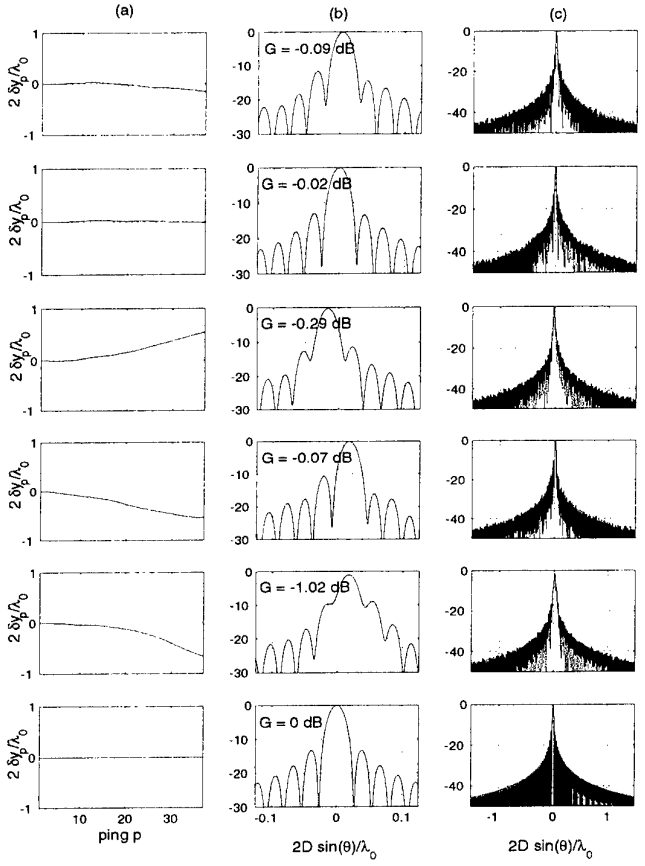


**Figure 8** *Simulated cross-track micronavigation errors $\delta y_p$ (a), corresponding SAS array factor beampatterns (b) and full SAS beampatterns (c), for $Q = 10$, $\alpha = 4$ and $\rho_{\text{eff}} = 35.4$ dB. In (b) are also indicated the normalized SAS array factor gains obtained in the realizations.*

The expected SAS gain, estimated by means of (20) by averaging over $10^6$ realizations, is equal to $\bar{G} = -0.235$ dB, in close agreement with the theoretical value of $\bar{G} = -0.25$ dB. The small discrepancy is attributed to approximation (25). The steering of the SAS array factor is apparent in Fig. 8(b), but it is seen to be of no consequence for the full SAS beampattern, as no grating lobes are visible at $\pm 1$ in Fig. 8(c).

The simulation also allows the estimation of the whole distribution of $G$ for given $Q$, $\alpha$ and $\rho_{\text{eff}}$. For $Q = 10$, $\alpha = 4$ and $\rho_{\text{eff}} = 35.4$ dB, the gain $G$ was found larger than $-0.84$ dB for 95% of the realizations.

### 6.2 Comparison with experiments

DPCA-micronavigated SAS results for a dual frequency 405/165 kHz sonar were presented in [6]. The experimental parameters of the 405 kHz SAS were $\alpha = 1.7$, $BW = 156$, $L_r/L_t = 29$, $\rho = 7.5$ dB. One has then $\rho_{\text{eff}} \simeq 44$ dB so that (41), with $\bar{G} = -0.25$ dB, gives a theoretical $Q$ of 14. According to [6], the $Q$ achieved experimentally was close to 9, although a direct experimental measure of the beampattern was not possible due to the absence of a strong point scatterer.

For the 165 kHz SAS, the experimental parameters were $\alpha = 1.8$, $BW = 156$, $L_r/L_t = 20$, $\rho = 6$ dB. One has then $\rho_{\text{eff}} \simeq 40.9$ dB giving now a theoretical $Q$ of 11.5. According to [6], the $Q$ achieved experimentally is close to 12. However, the experimental beampattern, measured for a spherical target, shows peak sidelobe levels only 4 dB below the main peak.

For the 100 kHz DPCA-micronavigated SAS discussed in [9], the data relative to Fig. 6 were obtained with $BW = 266$, $L_r/L_t = 45.6$, $\rho \cong 9.5$ dB and $\alpha \cong 4.3$, giving $\rho_{\text{eff}} = 50.4$ dB and a theoretical $Q$ of 29 to be compared to the value of $Q = 11$ obtained experimentally.

The above results show that the SAS performance obtained experimentally is usually significantly lower than the optimum theoretical performance, determined by the CRLBs. The origins of the discrepancy are as yet unexplained. Amongst the possible causes are residual calibration errors of the physical elements as well as approximations such as (5) and to a lesser extent (2).

The design of a 180/20 kHz DPCA-micronavigated SAS is presented in [5]. For the 180 kHz HFSAS the receive array is comprised of 11 elements spaced at 5 cm and the desired cross-range resolution up to a maximum range of 40 m is 2.5 cm, i.e., $Q = 24$ at the far range. For the 20 kHz LFSAS the receive array is comprised of 14 elements spaced at 7.5 cm and the desired cross-range resolution upto 40 m is 7.5 cm, i.e. $Q = 76$ at the far range. Both SAS are designed with only two elements in the DPCA, i.e., $K = 2$, giving $\alpha = 14/12$ for the 180 kHz HFSAS and $\alpha = 11/9$ for the 20 kHz LFSAS. It follows then from (41) that the required $\rho_{\text{eff}}$ is of the order of 64.4 dB for the HFSAS and 76.5 dB for the LFSAS.

Clearly obtaining such high values is challenging. The good experimental results obtained may be due to the fact that the HF/LFSAS is mounted on a very stable towbody. Assuming the towbody keeps a constant heading during the SAS integra-

tion time, the assumption that there is no yaw is valid so that (40), rather that (41), applies. The requirements in terms of $\rho_{\text{eff}}$ are then much more modest, of the order of 20.3 dB for the HFSAS and 20.7 dB for the LFSAS.

# 7
# Conclusions

The two most important parameters which govern the cross-range resolution gain $Q$ achievable by a DPCA-micronavigated SAS are:

1. the spatial oversampling factor $\alpha$,
2. the effective reverberation to noise ratio $\rho_{\text{eff}}$, defined as the product of the reverberation-to-noise ratio $\rho$, the number $L_r/L_t$ of independent elements in the receive aperture and the number $BW$ of independent temporal samples used in the estimation.

The achievable $Q$, for given $\rho_{\text{eff}}$, can be maximized by operating close to the optimum value of $\alpha$ which was shown to be $\alpha = 4$. The price to pay, however, is a reduction by a factor $\alpha$ of the area mapping rate.

The achievable $Q$ is limited chiefly by estimation errors on the heading of the physical array, which induce cross-track DPCA micronavigation errors of the SAS. Means of aiding DPCA in estimating this heading, such as additional instrumentation or new algorithms, would make possible higher resolution gains and increased mapping rates.

## Acknowledgments

The authors would like to thank L. S. Wang and R. Hollett for their useful remarks.

# References


[1] Cutrona, L. J. Comparison of sonar system performance achievable using synthetic-aperture techniques with the performance achievable by more conventional means. *Journal of the Acoustical Society of America*, **58**, 1975:336–346.

[2] Pinto, M. A., Fohanno, F., Trémois, O. and Guyonic, S. Autofocusing a synthetic aperture sonar using the temporal and spatial coherence of seafloor reverberation. *In:* Pace, N. G., Pouliquen, E., Bergem, O. and Lyons, A. P., *eds.* High Frequency Acoustics in Shallow Water, NATO SACLANTCEN, Lerici, Italy, 1997: pp 417-424. [ISBN 88-900194-1-7]

[3] Klemm, R. Space-Time Adaptive Processing, Principles and Applications. London, IEE, 1998.

[4] Doisy, Y. General motion estimation from correlation sonar. *IEEE Journal on Oceanic Engineering*, **23**, 1998: 127–140.

[5] Sammelmann, G. S., Fernandez, J. E., Christoff, J. T., Vaizer, L., Lathrop, J. D., Sheriff, R. W. and Montgomery, T. C. High frequency, low frequency synthetic aperture sonar. *Naval Research Reviews*, **49**, 1997: 3–8.

[6] Billon D. and Fohanno,F. Theoretical performance and experimental results for synthetic aperture sonar self-calibration. *In:* Proceedings of Oceans 98, Nice, 1998: pp 965–970.

[7] Pinto, M.A., Bellettini, A., Fioravanti, S., Chapman, S., Bugler, D. R., Perrot Y. and Hetet, A. Experimental investigations into high resolution sonar systems. *In:* Proceedings of Oceans 99, Seattle, 1999.

[8] Bellettini, A. and Pinto, M.A. Experimental investigation of synthetic aperture sonar micronavigation. *In:* Zacharia, M. E., *ed.*, Proceedings of the fifth European Conference on Underwater Acoustics ECUA 2000, Lyon, 10-13 July, 2000: pp 445–450. [ISBN 92-828-9530-0]

[9] Bellettini, A. and Pinto, M.A. Experimental results of a 100 kHz multi-aspect synthetic aperture sonar. *In:* Proceedings of the 5èmes Journées d'Etudes Acoustique Sous-Marine, Brest, 30 November–1 December, 2000.

[10] Jin, G. and Tang, D. Uncertainties of Differential Phase Estimation Associated with Interferometric Sonars. *IEEE Journal on Oceanic Engineering*, **21**, 1996: 53-63.

[11] Quazi, A.H. An overview on the time delay estimate in active and passive systems for target localization. *IEEE Transactions on Acoustics, Speech, and Signal Processing*, **29**, 1981: 527–533.

[12] Pinto M.A., Fioravanti, S., Bovio, E. Accuracy of synthetic aperture sonar micronavigation using a displaced phase centre antenna. Saclantcen Memorandum SM-352, 1999.

[13] Billon, D. and Pinto, M.A. Some general considerations for synthetic aperture sonar design. *In:* Proceedings of Oceans 95, San Diego, 1995: pp 1665-1670.

# Document Data Sheet

| Security Classification | | Project No. |
|---|---|---|
| UNCLASSIFIED | | 03-G |
| **Document Serial No.** | **Date of Issue** | **Total Pages** |
| SR-355 | February 2002 | 30 pp. |


**Author(s)**

Bellettini, A., Pinto, M.


**Title**

Accuracy of synthetic aperture sonar micronavigation using a displaced phase centre antenna: theory and experimental validation.


**Abstract**

The Cramér-Rao Lower Bounds (CRLBs) on the cross-track translation and rotation of a Displaced Phase Centre Antenna (DPCA) in the slant range plane between two successive pings (known as DPCA sway and yaw in what follows) are computed, assuming statistically homogeneous backscatter. These bounds are validated using experimental data from a 118-182 kHz sonar, showing an accuracy of the order of 20 microns on the ping-to-ping cross-track displacements.

Next, the accuracy required on the DPCA sway and yaw in order to achieve a given SAS beampattern specification, specified by the expected SAS array gain, is computed as a function of the number P of pings in the SAS. Higher accuracy is required when P increases to counter the accumulation of errors during the integration of the elementary ping-to-ping estimates: the standard deviation must decrease as $p^{1/2}$ for the DPCA sway and $p^{-3/2}$ for the yaw.

Finally, by combining the above results, the lower bounds on DPCA micronavigation accuracy are established. These bounds set an upper limit to the SAS length achievable in practice. The maximum gain Q in cross-range resolution achievable by a DPCA micronavigated SAS is computed as a function of the key SAS parameters. It is found that, for $P \gg 1$, the optimum SAS spatial sampling factor is 4, in the sense that it allows maximum Q. These theoretical predictions are compared with simulations and experimental results.



**Keywords**



**Issuing Organization**

North Atlantic Treaty Organization
SACLANT Undersea Research Centre
Viale San Bartolomeo 400, 19138 La Spezia, Italy

*[From N. America: SACLANTCEN (New York) APO AE 09613]*

Tel: +39 0187 527 361
Fax:+39 0187 527 700

E-mail: library@saclantc.nato.int